Finite Element Analysis and Design of Sandwich Panels Subject to Local Buckling Effects

Narayan Pokharel[1] and Mahen Mahendran[2]

ABSTRACT

Past research into the local buckling behaviour of fully profiled sandwich panels has been based on polyurethane foams and thicker lower grade steels. The Australian sandwich panels use polystyrene foam and thinner and high strength steels, which are bonded together using separate adhesives. Therefore a research project on Australian sandwich panels was undertaken using experimental and finite element analyses. The experimental study on 50 foam-supported steel plate elements and associated finite element analyses produced a large database for sandwich panels subject to local buckling effects, but revealed the inadequacy of conventional effective width formulae for panels with slender plates. It confirmed that these design rules could not be extended to slender plates in their present form. In this research, experimental and numerical results were used to improve the design rules. This paper presents the details of experimental and finite element analyses, their results and the improved design rules.

KEYWORDS

Profiled sandwich panels, slender plates, local buckling, buckling coefficient, effective width, finite element analysis.

[1] - PhD Research Scholar

[2] - Professor

School of Civil Engineering, Queensland University of Technology,

Brisbane, QLD 4000, Australia

1. INTRODUCTION

The use of sandwich panels in the construction of building structures offers many advantages as it leads to structures that are lightweight, cost effective and durable. The sandwich panels have been used as structural building components in many industrial and office buildings in Europe and the USA. Their use has now been extended to residential building construction due to their ability to improve the structural and thermal performance of the houses. Until recently sandwich panel construction in Australia has been limited to cold-storage buildings due to the lack of design methods and data. However, in recent times, the sandwich panels are increasingly used in building structures, particularly as roof and wall cladding systems.

Structural sandwich panels consist of two strong facings separated by and bonded rigidly to the centre core of lighter and weaker material. The steel faces of sandwich panels are generally used in three forms: flat, lightly profiled, and profiled. The faces of sandwich panels provide architectural appearance and structural stiffness, and protect the relatively vulnerable core material against damage or weathering. The faces take compressive and tensile loads and the core transfers shear loads between the faces while providing high bending stiffness. Hence, sandwich panels represent an excellent example of the optimum use of dissimilar materials.

Sandwich panels have flexible cores, and their behaviour is therefore more complex than that of the plain plates. Therefore it is important to understand the numerous failure modes of sandwich panels so that appropriate design criteria can be developed. The fully profiled sandwich panels are susceptible to local buckling effects under loading conditions such as direct compression, bending, or their combinations. Since the plate elements of the profiled sandwich panels are supported by foam core, their local buckling behaviour is significantly better than that of plate elements without foam core. Buckling of the panels may occur at a stress level lower than the yield stress of steel, but the panels, particularly those with low *b/t* ratios, will have considerable postbuckling strength. Such local buckling and postbuckling phenomena are very important in the design of sandwich panels.

During the last decade extensive research has been carried out in Europe and the USA to investigate the behaviour and design of sandwich panels for different failure conditions including that of local buckling effects of profiled sandwich panels. Davies (1987, 1993, 2001), Davies and Hakmi (1990, 1992), Davies and Heselius (1993), Davies et al. (1991) and Hassinen (1995) have investigated the local buckling behaviour and developed modified conventional effective width rules for the plate elements in sandwich panels. In their approach, current effective width rules (Winter, 1947) developed for the plain plate elements were extended to sandwich panels using the concept of a modified buckling coefficient. These design rules are included in the design document "European Recommendations for Sandwich Panels Part 1: Design" (CIB 2000).

However, these studies and design documents have been based on polyurethane foams and thicker steels of lower grade, and rely on some empirical factors. Moreover, these rules are commonly used for low width to thickness (*b/t*) ratios (< 200) of the plate elements (see

Figure 1). But in the sandwich panel construction, *b/t* ratios can be as large as 600 (Mahendran and Jeevaharan, 1999) because of the increasing use of thinner steels. Sandwich panels generally used in Australia comprise of thinner (0.42 mm) and high strength (minimum yield stress of 550 MPa and reduced ductility) steel faces and relatively thick polystyrene foam core which are bonded together using separate adhesives. Due to these limitations, current design documents are not used for Australian sandwich panels, particularly for those with higher plate slenderness. There is a need to verify the applicability of European recommendations to Australian panels in order to develop the confidence among Australian manufacturers and designers. Therefore a research project was conducted using a series of laboratory experiments and numerical analyses to study the local buckling behaviour of profiled sandwich panels made of thin high strength steel faces and polystyrene foam covering a wide range of *b/t* ratios.

In the first phase, a detailed experimental study on 50 foam-supported plate elements was conducted. The results showed that the conventional effective width formulae are adequate for sandwich panels with plate elements that have low *b/t* ratios, but not for panels with slender plate elements (Pokharel and Mahendran, 2001). To eliminate this problem and to improve the understanding of local buckling behaviour further, finite element analyses (FEA) of sandwich panels were undertaken using ABAQUS. Two different types of finite element models were developed and used in order to represent both the experimental sandwich panels and the more realistic sandwich panels used in building structures. Experimental results were used to calibrate the numerical models. Both FEA and experimental results were then used to review the current design rules. Based on the FEA results, a new improved design rule has been developed for the profiled sandwich panels considering their postbuckling behaviour.

This paper presents the details of the FEA models, their calibration using relevant experimental results, and the formulation of new design rules.

2. CURRENT DESIGN METHOD FOR LOCAL BUCKLING

In cold-formed steel design, *b/t* ratios are usually large and therefore local buckling becomes a major design criterion for compression members. Local buckling causes a loss of stiffness and redistribution of stresses, however considerable postbuckling strength exists that enables additional loads to be supported. Much of the load after buckling is carried by the regions of the plate near the edges. Thus only a fraction of the plate width is considered effective in resisting the applied compression load. Based on this, a simplified assumption has been developed that the maximum edge stress acts uniformly over two strips of plate and the central region is unstressed. This assumption has led to the development of effective width principles for the design of cold-formed steel members subject to local buckling effects. The original effective width formula for the plate elements was developed by Winter (1947) based on many tests and studies of postbuckling strength on light-gauge cold-formed steel plates and sections. This design formula is given by:

$$\left.\begin{aligned} & b_{eff} = \rho b \\ & \rho = \frac{1}{\lambda}\left[1 - \frac{0.22}{\lambda}\right] \text{ for } \lambda > 0.673 \\ & \rho = 1.0 \text{ for } \lambda \le 0.673 \\ & \lambda = 1.052\left[\frac{b}{t}\right]\sqrt{\frac{f_y}{E_f K}} \end{aligned}\right\} \qquad (1)$$

where f_y = yield stress, E_f = Young's modulus, t = plate thickness, K = buckling coefficient. The buckling coefficient K for the plate element without foam support is constant for a particular type of boundary conditions (eg. K = 4 for simply supported conditions). However, for the foam supported steel plate elements the K value changes with *b/t* ratios and mechanical properties of foam core and steel faces. Hence this effective width approach developed for plain plate elements has been extended to the profiled faces of sandwich panels by using the modified values of the buckling coefficient K (Davies and Hakmi, 1990).

The buckling coefficient K for sandwich panels can be determined theoretically by using energy principles in which the foam supported steel plate element can be considered as a plate on elastic foundation. Figure 2 shows a simply supported thin rectangular steel plate supported by a thick foam core representing an infinitely deep elastic half-space. The plate is subjected to an applied pressure p along the two transverse edges. The longitudinal edges of the plate are assumed to be simply supported. The length of the plate in x-direction is large compared with the width b. The critical buckling stress σ_{cr} evolves from an expression for the total potential energy of the plate element and the core.

$$\sigma_{cr} = \frac{K\pi^2 E_f}{12(1-\nu^2)(b/t)^2} \tag{2}$$

The buckling coefficient K can be determined by minimising the strain energy of the core in the expression of total potential energy with respect to K itself, and is given by (Davies and Hakmi, 1990):

$$K = \left[\frac{1}{\phi} + n^2\phi\right]^2 + R\phi\left[1 + n^2\phi^2\right]^{\frac{1}{2}} \tag{3}$$

where ϕ is a ratio of half-wave buckle length a to the width of the plate b ($\phi = a/b$), R is the dimensionless stiffness parameter which models the composite action between steel faces and foam core. When the stiffness of the core is zero (R = 0), Equation (3) represents the well known equation for the buckling of plain thin plates into square waves. For increasing values of R (R > 0), the critical value of half-wave buckle length a decreases with the increase in buckling coefficient K and thus raising the critical buckling stress σ_{cr}. An expression for R can be found by using half-space assumption and is expressed as (Davies and Hakmi, 1990):

$$R = \frac{24(1-\nu_f{}^2)(1-\nu_c)E_c}{\pi^3(1+\nu_c)(3-4\nu_c)E_f}\left[\frac{b}{t}\right]^3 \tag{4}$$

It can also be determined by using a simplified foundation model. If the simplified method is used, the alternative formula for R is given by:

$$R = \frac{12(1-\nu_f{}^2)}{\pi^3}\frac{\sqrt{E_c G_c}}{E_f}\left[\frac{b}{t}\right]^3 \tag{5}$$

where E_f and E_c are Young's modulus of steel faces and core, respectively, G_c is the shear modulus of foam core, ν_f and ν_c are the Poisson's ratios of steel face and foam core, respectively, b is the width and t is the plate thickness. The buckling coefficient K in Equation (3) can be minimised with respect to the wavelength parameter ϕ ($\partial K/\partial\phi = 0$) to determine the critical buckling stress σ_{cr}. Mathematically Equation (3) reduces to:

$$2n^4\phi - \frac{2}{\phi^3} + R(2n^2\phi^2+1)(n^2\phi^2+1)^{-\frac{1}{2}} = 0 \tag{6}$$

Using an appropriate numerical method, the value of ϕ can be determined from Equation 6. Using ϕ into Equation (3), K can be evaluated. However, this theoretical method of determining the buckling coefficient K has not been adopted in design processes as it is somewhat complicated. To simplify the practical design process, a number of explicit formulae have been proposed to determine K for sandwich panels with profiled faces. These formulae are given next.

Davies and Hakmi (1990) proposed the following equation to determine the buckling coefficient K for the design of sandwich panels. They indicated that this equation is accurate for a range of R from 0 to 200.

$$K=[16+11.8R+0.055R^2]^{1/2} \quad \text{with} \quad R=\frac{12(1-\nu_f{}^2)\sqrt{E_cG_c}}{\pi^3E_f}\left[\frac{b}{t}\right]^3 \tag{7}$$

Davies and Hakmi (1992) conducted a series of tests on thin-walled steel beams in which the compression flange was stiffened by foam to investigate the possibility of extending the effective width formula to sandwich panels. They found that Equation (7) is unsafe when compared with the test results for increasing values of *b/t* ratios. Following equation has therefore been proposed for K by replacing R in Equation (7) by $0.6R$.

$$K=[16+7R+0.02R^2]^{1/2} \tag{8}$$

Davies et al. (1991) proposed two equations for K based on half-space assumption and simplified foundation model. They are given next:

Based on half-space assumption,

$$K=4-0.415R+0.703R^2 \text{ with } R=\frac{b}{t}\left[\frac{E_c}{E_f}\right]^{1/3} \tag{9}$$

Based on simplified foundation model

$$K=4-0.474R+0.985R^2 \text{ with } R=\frac{b}{t}\left[\frac{E_cG_c}{E_f{}^2}\right]^{1/6} \tag{10}$$

Mahendran and Jeevaharan (1999) conducted a series of tests and finite element analyses on foam supported steel plate elements to investigate the local buckling behaviour. From this study, they proposed Equation (11) for K that can be applied for higher values of R up to 600.

$$K=[16+4.76R^{1.29}]^{1/2} \quad \text{with} \quad R=\frac{12(1-\nu_f{}^2)\sqrt{E_cG_c}}{\pi^3E_f}\left[\frac{b}{t}\right]^3 \tag{11}$$

In the current European Recommendations for Sandwich Panels, Part I: Design (CIB 2000), Equation (8) with the following R value has been recommended for predicting the value of K. These expressions are applicable for $0 \le R \le 200$ and $b/t \le 250$, and are based on an empirical reduction factor of $0.6R$ as recommended by Davies and Hakmi (1990).

$$K = [16 + 7R + 0.02R^2]^{1/2} \qquad \text{with} \quad R = 0.35\frac{\sqrt{E_c G_c}}{E_f}\left[\frac{b}{t}\right]^3 \tag{12}$$

3. EXPERIMENTAL INVESTIGATION

In the experimental investigation (Pokharel and Mahendran, 2001), 50 steel plate elements (25 each for G550 and G250 grade steels) supported by polystyrene foam cores as used in the profiled sandwich panels were tested under compression load. As the foam thickness has negligible effect on the buckling strengths (Mahendran and Jeevaharan 1999, Mahendran and McAndrew 2000), a constant thickness of 100 mm was used throughout the tests. To include a large range of *b/t* ratios (from 50 to 500), both the thickness and width of the plates were varied for each grade of steel (see Table 1). The lengths of the plates were chosen as three times the width (*b*) plus 10 mm for clamping. The steel faces and foam were glued to each other by using a suitable adhesive. The specimens were tested after 48 hours of attachment to ensure the adhesive was set and steel face and foam were joined properly. Details of the experimental program and test specimens are given in Table 1.

A specially constructed test rig was used to hold the test specimen with two vertical clamps allowing the vertical displacement and free rotation at the longitudinal edges, as required for the simply supported conditions. The test specimens were placed in the test rig between two loading blocks. The test set-up used in this investigation is similar to that used by Davies et al. (1991) at the technical research centre of Finland (VTT) for the investigation of the ultimate strength of compressed steel plates with and without core support. Researchers consider this test set-up using a simply supported plate element as a simplified model to study the local buckling problem of the faces of sandwich panels. A schematic diagram of the test rig is shown in Figure 3. The compression tests of the steel plate elements were carried out using a Tinius Olsen Testing Machine. A compression load was applied at a constant rate of 0.5 mm/min until the specimen failure. The buckling and ultimate loads of each test specimen were recorded. The buckling load was noted by visual observation of plate buckling whereas the maximum load carried by the specimen was taken as the ultimate load. Hence the buckling load was approximate, but the ultimate load could be considered exact. Further details of the experimental study are given in Pokharel and Mahendran (2001).

4. FINITE ELEMENT ANALYSIS

Local buckling behaviour of sandwich panels was investigated using a finite element program ABAQUS. The finite element model was based on the application of compressive load to one end of the steel face with all four sides of the plate being simply supported. The foam core was extended sufficiently deep to ensure that the theoretical approach of elastic half space (i.e. the core) to extend infinitely in this direction was simulated. To achieve this, a constant depth of 100 mm, same as in the experiments, was used for all the models.

The steel plate was modelled using S4R5 three dimensional thin shell elements with four nodes and five degree of freedom per node. Thin shell elements are normally used in cases where transverse shear flexibility is negligible and the thickness of the shell is less than about 1/15 of the characteristic length on the surface of the shell, such as the distance between the supports or the wave length of a significant eigenmode (HKS, 1998). Steel faces used in the sandwich panels fall well within this category and hence, 3D thin shell elements S4R5 with reduced integration were used to model them. The foam core was modelled using C3D8 three dimensional solid (continuum) elements with eight nodes and three degrees of freedom per node. These elements, which have no rotational degrees of freedom, are also called 8-node linear bricks. Since there was no relative movement between the steel faces and foam core, they were modelled as a single unit.

Measured material properties of polystyrene foam and steel faces were used in the analysis. They are E_c = 3.8 MPa, G_c = 1.76 MPa, ν_c = 0.08 for foam whereas the values for both G550 and G250 grades of steels are given in Table 1. The Poisson's ratio of steel was assumed to be ν = 0.3. Both materials were considered to be isotropic. A series of elastic buckling and non-linear analyses was undertaken using two different types of finite element models. The first model was the half-length experimental model analysed to calibrate with the experimental results whereas the second model was the half-wave buckle model analysed to simulate the real conditions of the sandwich panels used in building structures.

It is important that appropriate geometric imperfections and residual stresses are introduced in a finite element model while undertaking a non-linear analysis to simulate the true structural behaviour. However, residual stresses were not considered in the analysis of foam supported plate elements considered in this study as they did not involve welding or similar fabrication/manufacturing process capable of producing higher residual stresses. In the case of geometric imperfections, the mode shape based on the lowest eigenmode is sufficient to adequately characterize the most influential geometric imperfections, and this is considered an acceptable conservative approach (Schafer and Pekoz, 1998). Therefore, in the non-linear analyses of this study, the mode shape of the first buckling mode obtained from the elastic buckling analysis was used to introduce the critical geometric imperfection distribution shape.

Although the shape of geometric imperfection can be based on the eigenmodes from the buckling analysis, it is a very difficult task to determine the appropriate magnitude of geometric imperfection required to scale the imperfection distribution shape. Schafer and Pekoz (1998) recommended that the maximum value of geometric imperfection can be expressed in terms of plate width in the case of local buckling and in terms of thickness in the case of distortional buckling for cold-formed steel members without foam support. However, for sandwich panels, in which cold-formed steel plates are supported by a foam core, no data is available on the maximum value and the distribution of appropriate imperfection magnitudes to be used in numerical analyses. Experimentally it is impossible to measure the actual magnitudes of geometric imperfections in sandwich panels as they are quite small. It is obvious that the imperfection magnitude for thin steel faces supported by a foam core will not be as high as the values for flat plates without a foam core. Therefore, it is important to understand how the imperfections are produced in the manufacturing process. Through visits to sandwich panel manufacturing plants and extensive consultations with sandwich panel manufacturers, it was found that the width of the steel face has limited contribution to the geometric imperfection magnitude as the steel face is fully supported by foam core. However, it was observed that some imperfections might arise due to uneven surfaces of foam core, and their magnitudes would depend on the thickness of the steel plate used. Although this imperfection was very small, it might still cause some reduction to ultimate strength. Hence, in this study, the maximum imperfection value required for FEA was expressed in terms of the thickness of foam supported plate elements (t). A sensitivity analysis was conducted on a few sandwich panels with different plate thicknesses to determine the effects of maximum geometric imperfection. For a range of $0.1t$ to $0.4t$, reduction in ultimate strength due to these imperfections was found to be minimal (< 5%). As already described only a very small or no imperfections was observed in the sandwich panels produced by Australian manufacturers, it was decided to use 10% of plate thickness (0.1t) as the maximum value of geometric imperfections in all the finite element analyses.

4.1 Half Length Model

To simulate the foam-supported steel plate elements tested in the laboratory, a half-length model was used with appropriate boundary conditions including that of symmetry. In order to determine the appropriate mesh density, a convergence study was conducted with gradually increasing mesh size. On the basis of convergence study, a mesh with 10 mm square surface elements for steel plate and 10×10×5 mm solid elements throughout the foam depth was used. To confirm the results, a full length model was also analysed for some of the specimens. The length of the model used was 3 times the width as used in the experiments. Since the results from full length and half-length models agreed well, further analyses were conducted using half-length models with only half width to save on computational time. A constant foam thickness of 100 mm was used to simulate the experimental conditions (see Section 3).

Figure 4a shows the model geometry, mesh size and the loading pattern for half-length models. Appropriate boundary conditions were applied only to the steel face at the loading end and one of the longitudinal edges to simulate the experiments whereas symmetric boundary conditions were applied to the entire surface (i.e., to the steel faces and foam core) along both the longitudinal direction and across the width. The model was first analysed using an elastic buckling analysis. The first buckling mode which was very close to the experimental buckling mode was used to input geometric imperfections for the non-linear analysis. Figure 4b shows the buckled shape of the half-length model.

Elastic buckling and ultimate loads were obtained from buckling and non-linear analyses, respectively. These FEA results were compared with the corresponding experimental results. As seen in Table 2, the results from FEA and experiments agreed reasonably well for both G550 and G250 steel plates. The mean values of the ratio of FEA and experimental buckling and ultimate stresses were found to be 1.00 and 0.94, respectively, for G550 steel plates and 1.05 and 0.93, respectively, for G250 steel plates. The corresponding coefficients of variation (COV) were 0.06 and 0.11, respectively, for G550 steel plates and 0.08 and 0.12, respectively, for G250 steel plates. Figure 5 presents the comparison of typical load-deflection curves from FEA and experiments. Figure 6 presents the comparison of ultimate stress results from FEA with experiments. All these comparisons confirm that half-length FEA models can be successfully used to analyse the local buckling behaviour of foam-supported steel plate specimens used in the experiments.

Table 2 results for 0.42 mm and 0.60 mm G550 steel plates show slight reduction in experimental ultimate stresses compared with other plates. This is due to the limited ductility of thinner G550 steels associated with reduced strain hardening and fracture strain characteristics. To allow for this, Yang and Hancock (2002) have recommended the use of a reduced yield stress of $0.9f_y$ for G550 steels with a thickness less than 0.9 mm in member strength predictions. The finite element model used in this study did not simulate the effects of reduced ductility of thinner G550 grade steels and thus slightly over predicted the ultimate stress for such steel plates. However this research was continued using finite element models for both low and high strength steels as the aim of this research was to investigate the effects of plate slenderness on the strength of sandwich panels and not the effect of reduced ductility of G550 steel plates. It was considered that the latter effects are dealt with by using Yang and Hancock's (2002) recommendation.

4.2 Half Wave Buckle Length Model

The foam-supported steel plate elements used in the experiments do not represent exactly those in practical sandwich panels. For the simplicity of the experiments, foam width was made the same as the steel face width. In the test rig, only the steel plates were restrained along the four sides leaving the foam unrestrained, but the foam in sandwich panels is continuous along the width direction. Hence the half-length finite element model developed to simulate the experimental panels cannot be used for reviewing and developing the design rules for local buckling of sandwich panels. However, the validation of half-length model by comparing its results with the experimental results provided the confidence in using FEA model for developing design rules. The half-wave buckle length model matches with the theoretical model used to develop the buckling stress formula based on elastic half space method as given in Equations (2) to (6) (Mahendran and Jeevaharan, 1999). Hence a single half-wave buckle was modelled with appropriate boundary conditions including that of symmetry. A convergence study was conducted to determine the appropriate mesh size for half-wave buckle length models. A mesh with 10 mm square surface elements for steel plate and 10×10×5 mm solid elements throughout foam depth provided satisfactory results in terms of accuracy as in the case of the half-length model. However, to obtain more accurate results, a mesh with 5 mm square surface elements for steel plate and 5×5×5 mm solid elements throughout foam depth was used for half-wave buckle length models.

Appropriate boundary conditions were applied to the entire surface (i.e., to the steel faces and foam core) along all four sides. The length of the half-wave buckle length model, *a*/2, was found by varying *a*/2 using a series of elastic buckling analyses until the minimum buckling stress was obtained. The width of the model was *b*/2 (half the plate width), length *a*/2, and thickness sum of the steel thickness *t* and a constant foam thickness of 100 mm. The model geometry and the mesh used in the analyses are shown in Figure 7a. As in the case of half-length model, the half-wave buckle length model was analysed first using elastic buckling analysis, followed by a non-linear analysis. Figure 7b shows the buckled shape of the half-wave buckle length model.

The half-wave buckle length *a* and critical buckling load were obtained from elastic buckling analyses whereas the ultimate failure load was obtained from non-linear analyses. The half-wave buckling length *a* and the critical buckling load were compared with the theoretical results obtained from Equations (2) to (6). Tables 3 and 4 present the comparison of these buckling results from FEA and theory along with the ultimate loads obtained from the FEA for G550 steel plates and G250 steel plates, respectively. As seen from these results, both half-wave buckle length *a* and critical buckling loads from FEA agreed reasonably well with the theoretical results. The mean and COV of the ratio of buckling loads from FEA and theory was found to be 0.97 and 0.01, respectively, for G550 steel plates, and 0.90 and 0.03, respectively, for G250 steel plates. Hence these agreements confirm that the half-wave buckle length model can be successfully used to model the local buckling behaviour, review the existing design rules, understand the inadequacy of current effective width approach for slender plates, and develop new improved design formulae.

5. COMPARISON OF EFFECTIVE WIDTH RESULTS

Effective widths of foam supported steel plate elements were determined from the FEA ultimate stresses given in Tables 3 and 4 using b_{eff}/b = ultimate stress/yield stress. These effective widths obtained from FEA results and those evaluated from Equation (1) using K values predicted by theory and different buckling formulae are plotted against the b/t ratios in Figures 8(a) and (b) for G550 steel plates and G250 steel plates, respectively. The buckling coefficients (K) were determined for the foam-supported steel plate elements by using Equations (7), (11) and (12) as proposed by Davies and Hakmi (1990), Mahendran and Jeevaharan (1999) and CIB (2000), respectively. Theoretical values of K were determined by using Equations (3) to (6). It can be observed from Figures 8(a) and (b) that the effective widths (b_{eff}) evaluated from Equation (1) using K values predicted by theory and different buckling formulae agreed reasonably well with the FEA results for low b/t ratios (< 100). However, for higher b/t ratios, all the formulae predicted very high effective width values compared with the FEA results. FEA results clearly indicated that none of the formulae could estimate reasonable values of effective width for slender plates with high b/t ratios (> 100).

Hence the detailed finite element analyses along with experimental investigations clearly showed and confirmed that the current design formulae are not applicable for slender plates. This implies the inadequacy of conventional effective width formulae. It is worth noting here that the original effective width formula (Equation 1) for the plain plate elements was developed by Winter (1947) based on many tests and studies on light-gauge cold-formed steel sections considering the postbuckling behaviour of plain plates alone. But foam-supported steel plate element is a composite unit made of steel plate and foam core. While dealing with such cases, postbuckling behaviour of composite as a whole should be taken into account for developing design rules for sandwich panels. Further, since the buckling coefficient *K* for the plate element without foam support is constant for a particular type of boundary conditions (eg. $K = 4$ for simply supported conditions), a constant value of *K* was used in developing Equation (1). By simply changing the *K* value, the formulae can be extended to other types of boundary conditions. However, the buckling coefficient *K* is not a constant parameter for sandwich panels. It changes with *b/t* ratios and mechanical properties of foam and steel plates. Further, the plate elements with high *b/t* ratios have very little or no postbuckling strength. Therefore a simple extension of effective width approach based on the postbuckling strength of sandwich panels with slender plates may not represent the true ultimate strength behaviour. If the *b/t* ratio of the plate element is very high, the strength will be governed by wrinkling failure and can be determined by the well established wrinkling formula (CIB 2000). A finite element study conducted on foam supported plate elements with very low to very high b/t ratios has confirmed that the wrinkling failure is more dominant for plates with *b/t* ratio greater than 1000. The plate elements with *b/t* ratios in the range of 250 to 1000 show little or no postbuckling strength. However, the panels in this range do not fail by wrinkling as their ultimate strength is higher than wrinkling stress. Therefore this intermediate region can still be considered as a local buckling region despite the lack of significant postbuckling strength. Plate elements in many fully profiled sandwich panels belong to this region as the *b/t* ratios of these plate elements are in the range of about 30 to 600. Therefore the wrinkling formula should not be used for the plate elements in profiled sandwich panels as it will underestimate the true strength of the panel. An alternative design equation which can be successfully applied for a wider range of *b/t* ratio including this intermediate region has to be developed to ensure accurate designs of sandwich panels.

From the FEA and experimental findings on foam supported steel plates, it can be concluded that the current effective width approach can not be extended to the sandwich panels with slender plates in its present form. New improved design formulae have to be developed based on the finite element analysis results to estimate accurate values of effective widths that can be used for design purposes. To achieve this objective, the FEA results for all the specimens were evaluated and further FEA were undertaken to include *b/t* ratios from 30 to 600. This produced a large database covering a wider range of *b/t* ratios for sandwich panels subject to local buckling effects. Based on these FEA results, an improved design equation has been formulated as described next.

6. DEVELOPMENT OF NEW DESIGN RULES

Investigation of local buckling behaviour of foam-supported steel plate elements with simply supported longitudinal edges is an essential preliminary step towards the development of design rules for profiled sandwich panels. Section 2 of the paper presents the details of the local buckling behaviour and current design approaches based on effective widths. Figure 9 illustrates the redistribution of the stress across the plate width after buckling and the concept of effective width. As seen in this figure, the redistribution of stress continues until the stress at the edges reaches the yield point (f_y) of the steel and then the plate begins to fail.

Effective width b_{eff} is considered as a particular width of the foam supported steel plate which just buckles when the compressive stress reaches the yield point of the steel. Using this assumption, the value of b_{eff} can be determined using the following formula (Yu, 2000):

$$\sigma_{cr} = f_y = \frac{K\pi^2 E_f}{12(1-\nu^2)(b_{eff}/t)^2} \tag{13}$$

$$b_{eff} = \sqrt{K}\sqrt{\frac{\pi^2}{12(1-\nu^2)}}\, t\sqrt{\frac{E_f}{f_y}} = \sqrt{K}Ct\sqrt{\frac{E_f}{f_y}} \tag{14}$$

where

$$C = \sqrt{\frac{\pi^2}{12(1-\nu^2)}} = 0.95 \quad \text{(assuming } \nu = 0.3\text{)} \tag{15}$$

Before buckling, the width of the plate is fully effective and hence the critical buckling stress can be determined by using the full width *b* as follows:

$$\sigma_{cr} = \frac{K\pi^2 E_f}{12(1-\nu^2)(b/t)^2} \tag{16}$$

$$b = \sqrt{K}\sqrt{\frac{\pi^2}{12(1-\nu^2)}}\; t\sqrt{\frac{E_f}{\sigma_{cr}}} = \sqrt{K}Ct\sqrt{\frac{E_f}{\sigma_{cr}}} \tag{17}$$

Taking the ratio of Equations (14) and (17), the relation between b_{eff} and b can be established as:

$$\frac{b_{eff}}{b} = \sqrt{\frac{\sigma_{cr}}{f_y}} \tag{18}$$

Equations (14) and (15) are the von Karman formulae for the design of stiffened elements developed in 1932. However, experimental investigations by Sechler (1933) and Winter (1947) showed that the term C used in Equation (14) depends primarily on the non-dimensional parameter γ expressed in the following way (Yu, 2000):

$$\gamma = \sqrt{\frac{E_f}{f_y}}\left(\frac{t}{b}\right) \tag{19}$$

From Equation (14), the term C can be rewritten as:

$$C = \frac{b_{eff}}{t}\sqrt{\frac{f_y}{KE_f}} \tag{20}$$

From the finite element analysis conducted in this study, effective widths b_{eff} of foam supported plate elements were determined based on the ultimate stresses. Using Equation (20), the term C was evaluated for all the specimens considered. The corresponding non-dimensional parameter γ was determined using Equation (19). A graph was plotted to establish the relationship between C and γ as shown in Figure 10. The following Equation has been developed for the term C based on the finite element analysis results.

$$C = 0.322(1 + 7.32\gamma - 11.48\gamma^2 + 4.59\gamma^3) \tag{21}$$

Substituting the value of γ into Equation (21),

$$C = 0.322(1 + 7.32\left(\frac{t}{b}\right)\left(\frac{E_f}{f_y}\right)^{1/2} - 11.48\left(\frac{t}{b}\right)^2\left(\frac{E_f}{f_y}\right) + 4.59\left(\frac{t}{b}\right)^3\left(\frac{E_f}{f_y}\right)^{3/2} \tag{22}$$

By substituting the value of C in Equation (14), a modified formula for computing the effective width b_{eff} for foam supported plate elements can be obtained.

$$\rho = \frac{b_{eff}}{b} = \frac{0.34}{\lambda}\left[1 + \frac{7.71}{\beta} - \frac{12.72}{\beta^2} + \frac{5.35}{\beta^3}\right] \tag{23}$$

where

$$\lambda = 1.052\left[\frac{b}{t}\right]\sqrt{\frac{f_y}{E_f K}} \tag{24}$$

$$\beta = 1.052\left[\frac{b}{t}\right]\sqrt{\frac{f_y}{E_f}} \tag{25}$$

if
$$\left.\begin{array}{ll} \rho \geq 1, & b_{eff} = b \\ \rho < 1, & b_{eff} = \rho b \end{array}\right\} \tag{26}$$

Alternatively, a simpler design formula with slightly reduced accuracy can be developed based on the same procedure as mentioned above. This is given next and can be used instead of Equation (23).

$$\rho = \frac{b_{eff}}{b} = \frac{0.355}{\lambda}\left[1 + \frac{6.44}{\beta} - \frac{7.89}{\beta^2}\right] \tag{27}$$

7. VALIDATION OF NEW DESIGN RULES

From the series of experimental and FEA results, it was concluded that conventional effective width formula developed for plain steel plates can not be extrapolated to the foam supported plate elements with higher plate slenderness. Hence, improved design formulae as given in Equations (23) to (26) have been developed by considering the local and postbuckling behaviour of the composite sandwich panel plate elements.

To examine the reliability and accuracy of the new design rules, the effective widths for different grades (G550 and G250) of foam supported steel plate elements obtained from finite element analysis were compared with the predictions from Equation (23). The effective width results are plotted against *b/t* ratios in Figures 11(a) and (b) for G550 steel plates and G250 steel plates, respectively. From these figures it can be observed that the predicted values are in very good agreement with the FEA results for a very large range of *b/t* ratios. The new design equation can predict accurate values of effective widths for any plate slenderness simulating that of compact plates with very low b/t ratios to slender plates with very high b/t ratios (600). Hence these comparisons confirm that the new design formula can be used for the design of profiled sandwich panels subject to local buckling effects.

8. CONCLUSIONS

An extensive series of experiments and finite element analyses was conducted to investigate the local buckling behaviour of foam supported steel plate elements. Appropriate finite element models were developed to simulate the behaviour of foam-supported steel plate elements used in the laboratory experiments as well as sandwich panels used in various building structures. The finite element model was validated using experimental results and then used to review the current design rules. The results reveal the inadequacy of using the conventional effective width approach. It is concluded that for low *b/t* ratios (<100) current effective width design rules can be applied, but for slender plates these rules can not be extended in their present form. Based on the results from this study, an improved design equation has been developed considering the local buckling and postbuckling behaviour of sandwich panels for a large range of *b/t* ratios (<600) for design purposes.

9. REFERENCES

1. Davies, J.M. (1987). Design Criteria for Structural Sandwich Panels. *Journal of Structural Engineering* 65A (12), pp. 435-441.
2. Davies, J.M. (1993). Sandwich Panels. *Thin-Walled Structures*, 16, pp.179-198.
3. Davies, J.M. (2001). *Light Weight Sandwich Construction*, Blackwell Science, UK
4. Davies, J.M. and Hakmi, M.R. (1990). Local Buckling of Profiled Sandwich Plates. *Proc. IABSE Symposium, Mixed Structures including New Materials*, Brussels, September, pp. 533-538.
5. Davies, J.M. and Hakmi, M.R. (1992). Postbuckling Behaviour of Foam-Filled Thin-Walled Steel Beams. *Journal of Construction Steel Research*, 20, pp. 75-83.
6. Davies, J.M., Hakmi, M.R. and Hassinen, P. (1991). Face Buckling Stress in Sandwich Panels. *Proc*. *Nordic Steel Colloquium*, pp. 99-110.
7. Davies, J.M. and Heselius, L. (1993). Design Recommendations for Sandwich Panels. *Journal of Building Research and Information*, 21(3), pp. 157-161.
8. Hassinen, P. (1995). Compression Failure Modes of Thin Profiled Metal Sheet Faces of Sandwich Panels, *Sandwich Construction 3-Proceedings of the Third International Conference*, Southampton, pp. 205-214.
9. Hibbitt, Karlsson and Sorensen, Inc., (HKS) (1998). *Abaqus User's Manual*, Pawtucket, RI, USA.

10. International Council for Building Research, Studies and Documentation (CIB) (2000) *European Recommendations for Sandwich Panels Part 1: Design*, CIB Publication 147.

11. Mahendran, M. and Jeevaharan, M. (1999). Local Buckling Behaviour of Steel Plate Elements Supported by a Plastic Foam Material. *Structural Engineering and Mechanics*, 7(5), pp. 433-445.

12. Mahendran, M. and McAndrew, D. (2000). Flexural Wrinkling Behaviour of Lightly Profiled Sandwich Panels. *Proc. 15th Int. Specialty Conf. on Cold-formed Steel Structures*, St. Louis, USA, pp. 563-576.

13. Pokharel, N. and Mahendran, M. (2001). Local Buckling Behaviour of Sandwich Panels. *Proc. Third International Conference on Thin-Walled Structures*, Krakow, Poland, 5-7 June 2001, pp. 523 – 530.

14. Schafer, B.W. and Pekoz, T (1998). Computational Modelling of Cold-Formed Steel: Characterizing Geometric Imperfections and Residual Stresses. *Journal of Constructional Steel Research* 47, pp. 193 – 210.

15. Sechler, E.E. (1933). The Ultimate Strength of Thin Flat Sheet in Compression. Publication 27, Guggenhein Aeronautics Laboratory, California Institute of Technology, Pasadena.

16. Winter, G. (1947). Strength of Thin Steel Compression Flanges. Trans. ASCE, Vol 112, pp. 527.

17. Yu, W. (2000). *Cold-Formed Steel Design*, John Wiley and Sons, Inc., 3rd Edition, USA.

18. Yang, D. and Hancock, G.J. (2002). Compression Test of Cold-Reduced High Strength Steel Stub Columns. *Research Report No R815*, The University of Sydney, Australia.

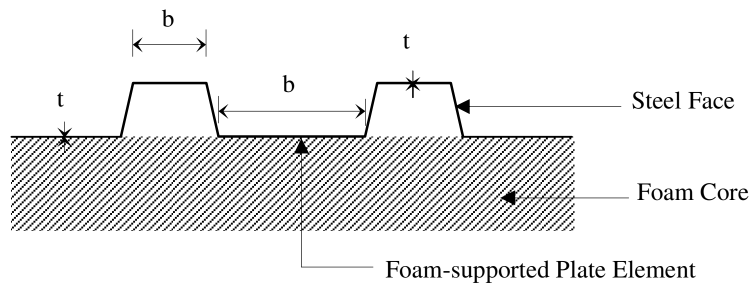

Figure 1: Critical *b/t* Ratios of Profiled Sandwich Panels for Local Buckling

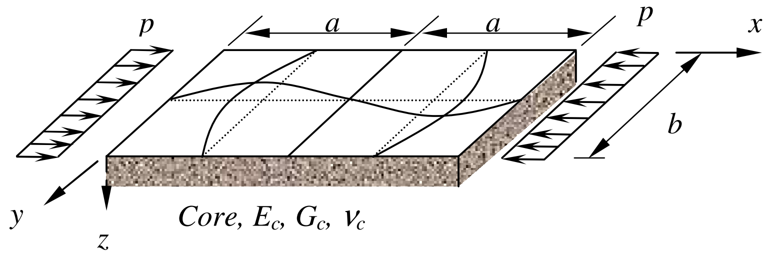

Figure 2: Steel Plate in Compression with Core as an Elastic Foundation

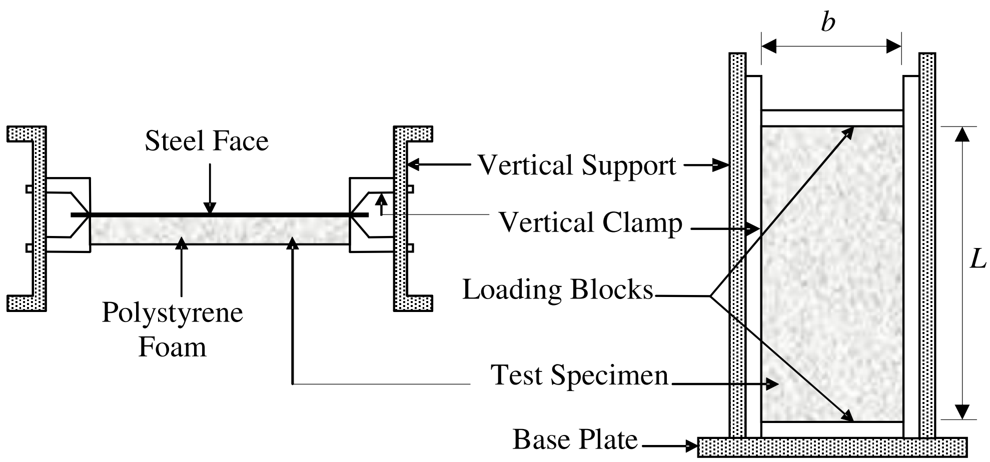

Figure 3: Schematic Diagram of Test Rig

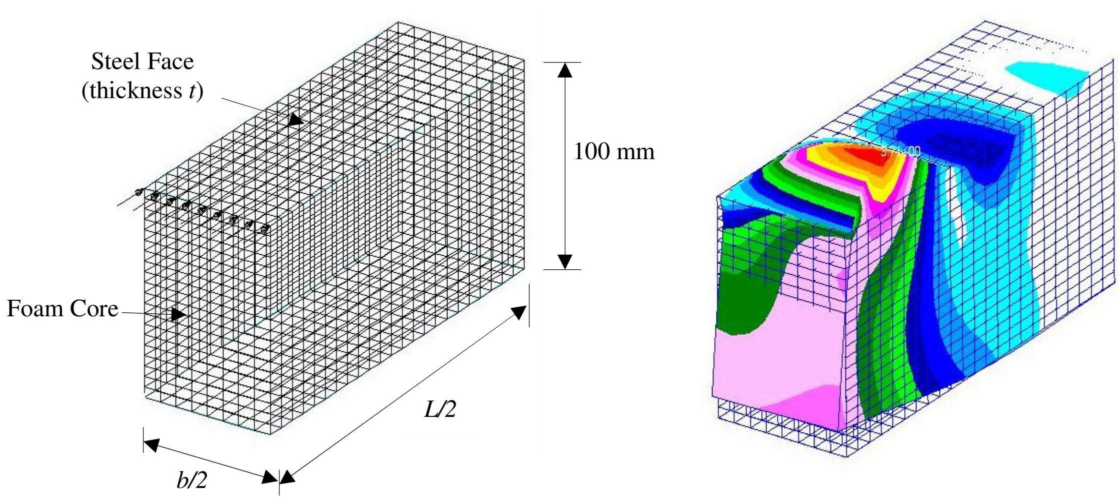

(a) Model (b) Buckle shape

Figure 4: Half-Length FEA Model Simulating Experimental Steel Plates Supported by Foam Core

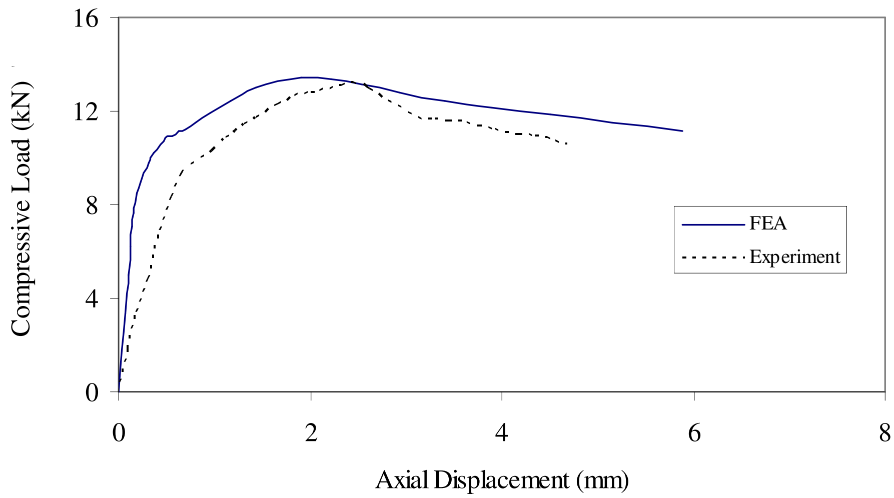

(a) Compressive Load vs Axial Displacement

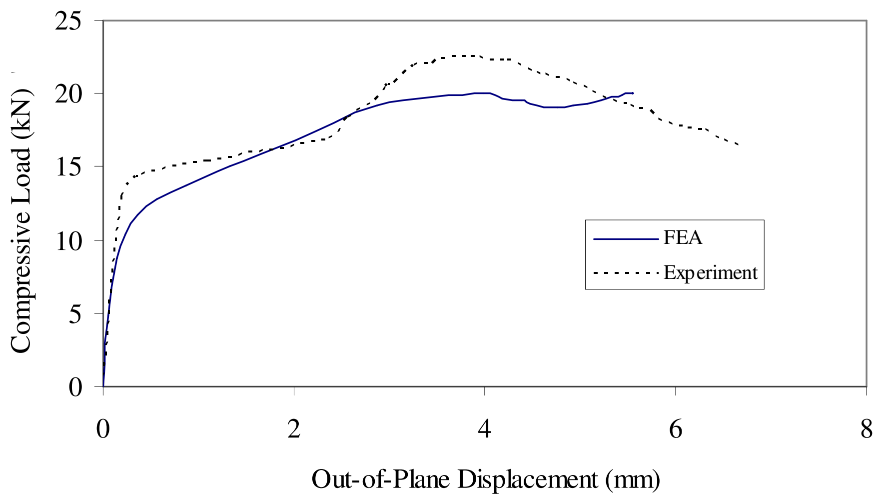

(b) Compressive Load vs Out-of-Plane Displacement

Figure 5: Comparison of Typical Load-Deflection Curves from FEA and Experiments

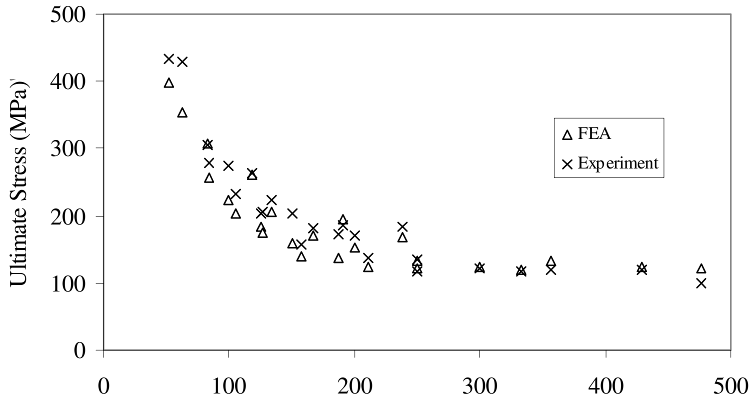

(a) G550 Steel

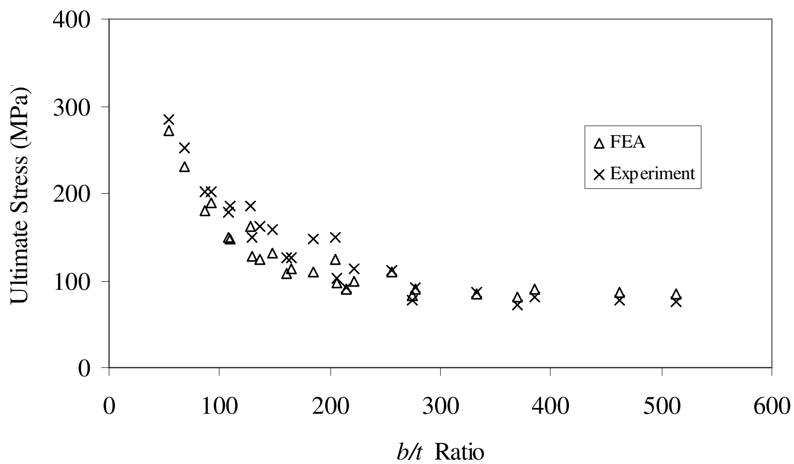

(b) G250 Steel

Figure 6: Comparison of FEA and Experimental Ultimate Stress Results

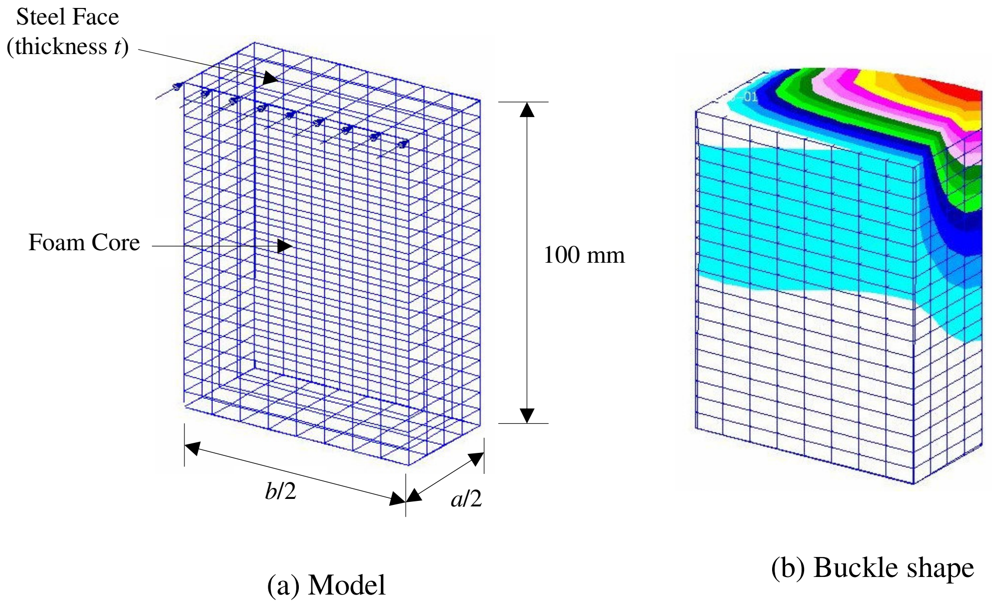

Figure 7: Half-Wave Buckle Length Model of Steel Plate Supported by Foam Core

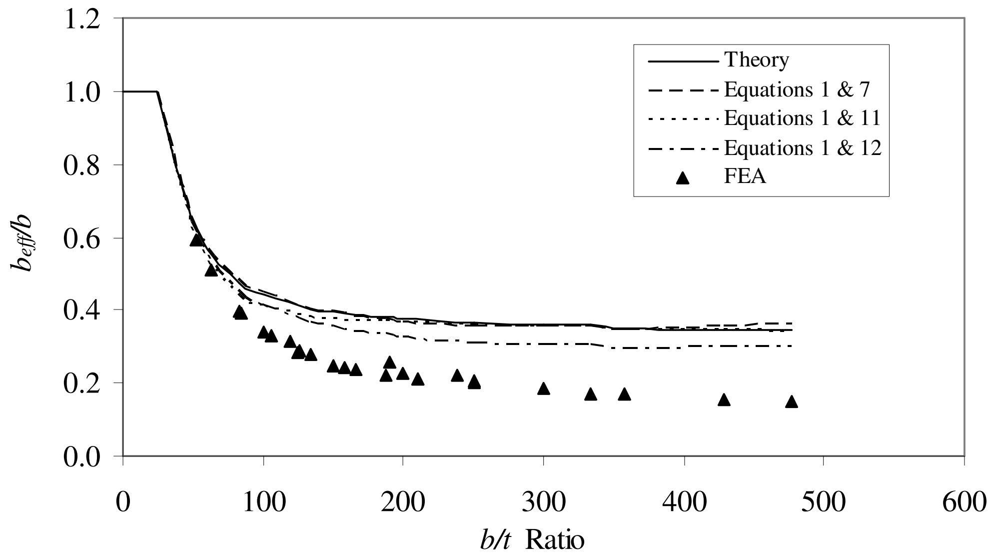

(a) G550 Steel

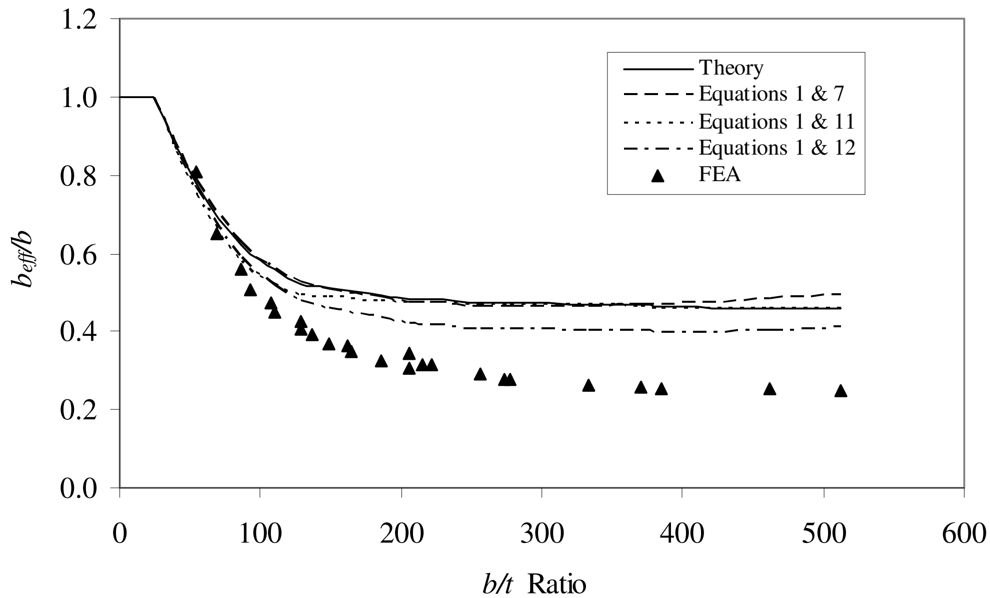

(b) G250 Steel

Figure 8: Effective Width of Steel Plate Elements Supported by Foam Core

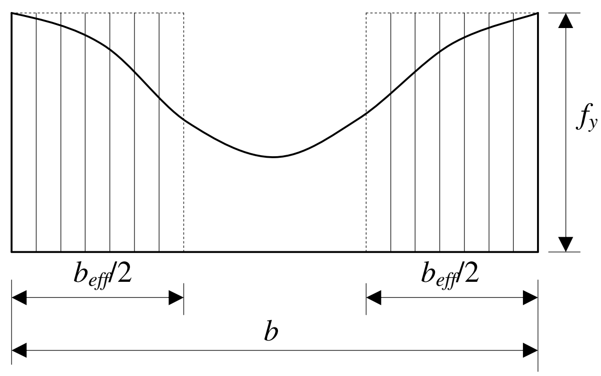

Figure 9: Definition of Effective Width of Foam Supported Steel Plate Element

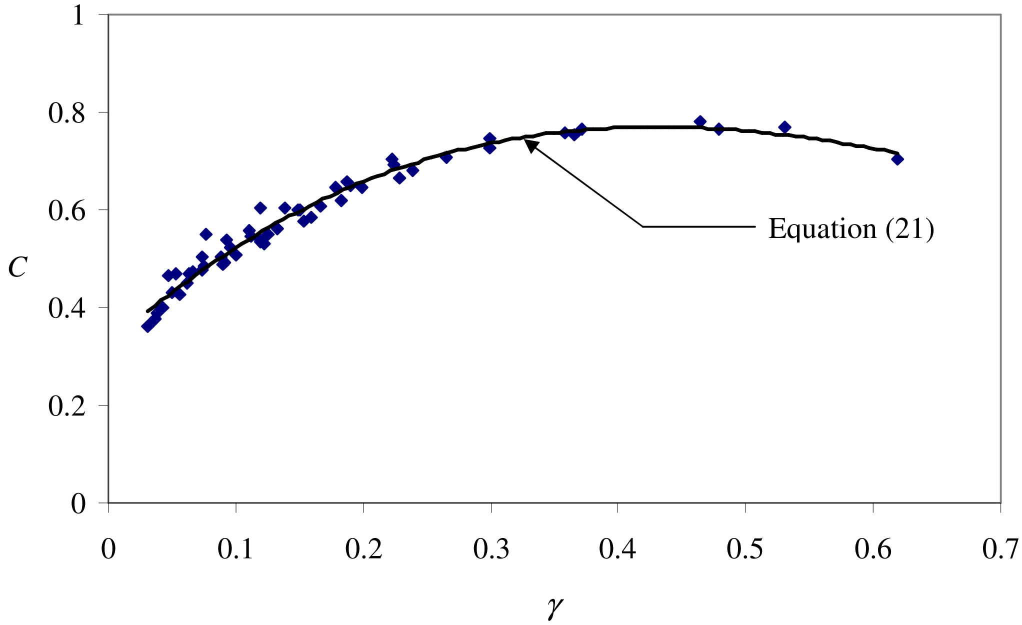

Figure 10: Deriving an Expression for *C*

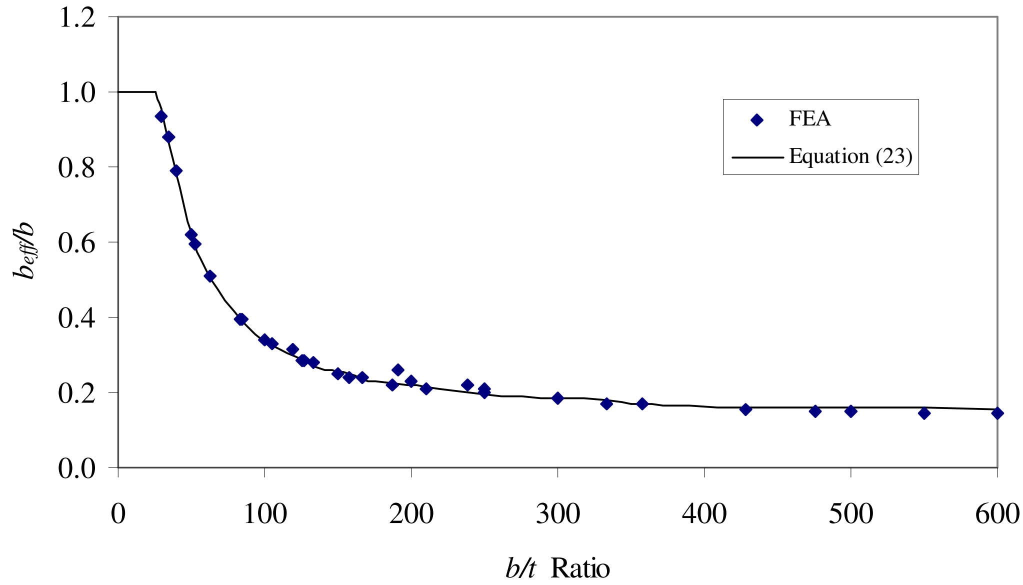

(a) G550 Steel

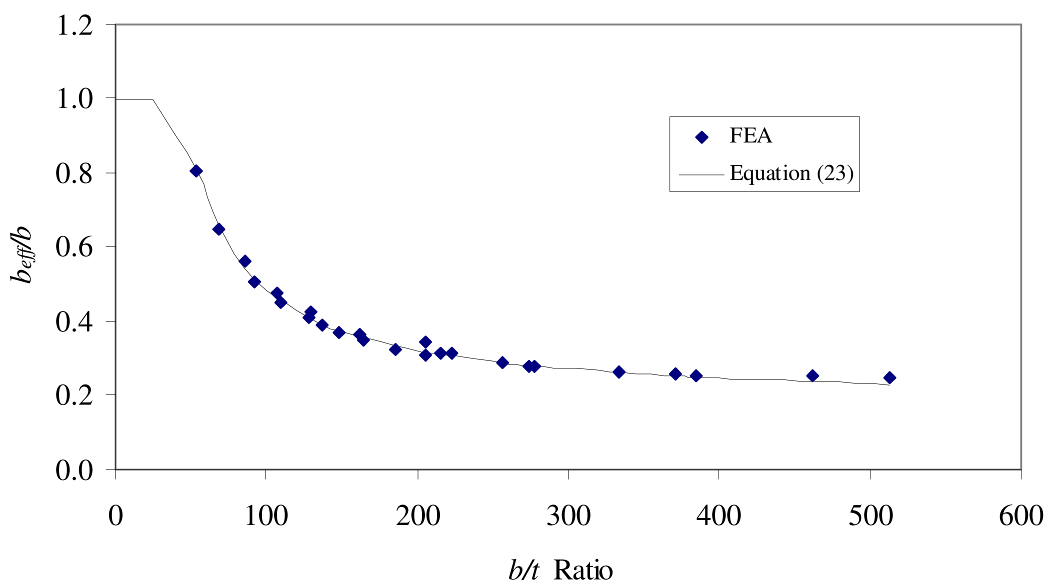

G250 Steel

Figure 11: Effective Widths from FEA and New Design Equations

Table 1: Experimental Program

Test series	Plate width b (mm)	G550 steel plates					G250 steel plates				
		Thickness (mm)		Measured		b/t ratio	Thickness (mm)		Measured		b/t ratio
		Spec.	bmt	f_y (MPa)	E_f (GPa)		Spec.	bmt	f_y (MPa)	E_f (GPa)	
1	50	0.95	0.95	637	226	52.6	1.00	0.93	326	216	53.8
2	50	0.80	0.80	656	230	62.5	0.80	0.73	345	217	68.5
3	50	0.60	0.60	682	235	83.3	0.60	0.54	360	218	92.6
4	50	0.42	0.42	726	239	119.0	0.40	0.39	368	220	128.2
5	80	0.95	0.95	637	226	84.2	1.00	0.93	326	216	86.0
6	80	0.80	0.80	656	230	100.0	0.80	0.73	345	217	109.6
7	80	0.60	0.60	682	235	133.3	0.60	0.54	360	218	148.1
8	80	0.42	0.42	726	239	190.5	0.40	0.39	368	220	205.1
9	100	0.95	0.95	637	226	105.3	1.00	0.93	326	216	107.5
10	100	0.80	0.80	656	230	125.0	0.80	0.73	345	217	137.0
11	100	0.60	0.60	682	235	166.7	0.60	0.54	360	218	185.2
12	100	0.42	0.42	726	239	238.1	0.40	0.39	368	220	256.4
13	120	0.95	0.95	637	226	126.3	1.00	0.93	326	216	129.0
14	120	0.80	0.80	656	230	150.0	0.80	0.73	345	217	164.4
15	120	0.60	0.60	682	235	200.0	0.60	0.54	360	218	222.2
16	150	0.95	0.95	637	226	157.9	1.00	0.93	326	216	161.3
17	150	0.80	0.80	656	230	187.5	0.80	0.73	345	217	205.5
18	150	0.60	0.60	682	235	250.0	0.60	0.54	360	218	277.8
19	150	0.42	0.42	726	239	357.1	0.40	0.39	368	220	384.6
20	180	0.60	0.60	682	235	300.0	0.60	0.54	360	218	333.3
21	180	0.42	0.42	726	239	428.6	0.40	0.39	368	220	461.5
22	200	0.95	0.95	637	226	210.5	1.00	0.93	326	216	215.1
23	200	0.80	0.80	656	230	250.0	0.80	0.73	345	217	274.0
24	200	0.60	0.60	682	235	333.3	0.60	0.54	360	218	370.4
25	200	0.42	0.42	726	239	476.2	0.40	0.39	368	220	512.8

Note: f_y – measured yield stress of steel, E_f – measured Young's modulus

b/t ratio – plate width *b/bmt*, Spec. – specified thickness

bm*t* – estimated base metal thickness based on measured total coated thickness

Table 2: Comparison of FEA Results based on Half-Length Model with Experimental Results

Test No.	G550 Steel Plates					G250 Steel Plates				
	b/t ratio	Buckling stress (MPa)		Ultimate stress (MPa)		b/t ratio	Buckling stress (MPa)		Ultimate stress (MPa)	
		FEA	Expt.	FEA	Expt.		FEA	Expt.	FEA	Expt.
1	52.6	352.8	336.2	397.5	434.3	53.8	327.7	272.5	271.2	285.4
2	62.5	275.0	293.0	353.0	428.3	68.5	232.1	221.9	231.2	251.5
3	83.3	196.0	238.3	308.3	305.0	92.6	167.4	151.9	188.5	201.5
4	119.0	138.6	141.9	260.0	264.3	128.2	125.1	146.7	162.6	186.2
5	84.2	182.2	170.3	257.1	279.2	86.0	172.6	171.2	180.9	201.6
6	100.0	153.1	155.8	223.0	275.0	109.6	134.6	152.6	148.1	185.4
7	133.3	121.3	112.9	205.0	223.3	148.1	110.0	98.1	132.2	159.0
8	190.5	103.3	97.0	194.0	186.0	205.1	97.4	88.1	124.0	149.0
9	105.3	140.6	139.4	203.3	232.6	107.5	133.8	123.4	149.6	178.1
10	125.0	122.5	132.8	182.9	203.4	137.0	111.8	121.4	123.6	162.1
11	166.7	105.0	102.0	171.3	181.8	185.2	97.0	90.9	110.4	148.1
12	238.1	93.6	87.6	167.6	184.0	256.4	89.2	76.9	109.2	111.3
13	126.3	118.4	122.1	174.6	205.2	129.0	113.7	119.4	128.5	150.2
14	150.0	107.4	119.8	159.1	203.5	164.4	99.5	98.6	113.0	126.4
15	200.0	95.1	91.0	152.2	169.9	222.2	89.0	85.2	99.4	113.3
16	157.9	101.1	104.6	140.4	158.1	161.3	97.7	96.8	108.7	125.5
17	187.5	93.9	96.1	138.3	172.8	205.5	88.3	87.2	96.5	101.9
18	250.0	86.1	83.9	133.2	133.9	277.8	81.5	76.5	89.4	91.2
19	357.1	81.1	79.0	133.3	119.2	384.6	78.1	67.2	90.6	80.3
20	300.0	80.5	78.6	124.4	122.6	333.3	76.7	73.6	84.7	86.0
21	428.6	77.1	77.8	124.9	118.4	461.5	74.6	64.1	86.6	78.3
22	210.5	86.2	88.2	124.3	136.5	215.1	83.8	84.9	89.8	91.6
23	250.0	82.1	79.9	122.0	117.1	274.0	78.3	72.7	82.7	78.0
24	333.3	77.7	71.4	118.5	118.0	370.4	74.3	65.7	81.7	71.9
25	476.2	75.0	80.0	120.6	100.1	512.8	72.7	64.6	84.0	75.6

Table 3: Comparison of FEA Results based on Half-Wave Buckle Length Model with Theoretical Results for G550 Steel Plates

Test series	b/t ratio	a/b ratio		Buckling stress (MPa)		Buckling stress ratio	Ultimate stress (MPa)
		Theory	FEA	Theory	FEA	FEA/Theory	FEA
1	52.6	0.884	0.88	350.3	350.9	1.00	377.5
2	62.5	0.834	0.84	275.8	274.8	1.00	334.0
3	83.3	0.727	0.72	196.7	194.3	0.99	270.3
4	119.0	0.576	0.60	146.7	143.3	0.98	228.6
5	84.2	0.718	0.73	189.5	185.0	0.98	250.3
6	100.0	0.646	0.65	163.3	158.8	0.97	223.0
7	133.3	0.526	0.55	135.6	130.8	0.96	189.6
8	190.5	0.393	0.40	117.6	113.4	0.96	188.7
9	105.3	0.621	0.64	155.1	149.9	0.97	210.5
10	125.0	0.550	0.56	139.1	134.0	0.96	187.3
11	166.7	0.439	0.46	122.2	117.2	0.96	162.3
12	238.1	0.322	0.34	111.0	106.7	0.96	161.0
13	126.3	0.544	0.57	137.0	131.6	0.96	182.9
14	150.0	0.476	0.48	126.5	121.1	0.96	162.9
15	200.0	0.375	0.38	115.0	110.0	0.96	155.4
16	157.9	0.454	0.47	122.6	117.1	0.95	154.4
17	187.5	0.394	0.41	116.2	110.9	0.95	143.8
18	250.0	0.306	0.32	109.2	104.3	0.96	141.9
19	357.1	0.220	0.23	104.6	100.6	0.96	122.7
20	300.0	0.259	0.27	106.1	101.3	0.95	124.7
21	428.6	0.185	0.19	103.2	99.2	0.96	113.0
22	210.5	0.354	0.37	111.6	105.9	0.95	133.4
23	250.0	0.304	0.32	108.3	103.1	0.95	132.6
24	333.3	0.234	0.24	104.8	100.0	0.95	117.1
25	476.2	0.167	0.17	102.5	98.6	0.96	108.9

Table 4 Comparison of FEA Results based on Half-Wave Buckle Length Model with Theoretical Results for G250 Steel Plates

Test Series	b/t Ratio	a/b Ratio		Buckling Stress (MPa)			Ultimate Stress (MPa)
		Theory	FEA	Theory	FEA	Ratio FEA/Theory	
1	53.8	0.873	0.88	350.8	326.2	0.93	262.8
2	68.5	0.795	0.80	255.6	231.5	0.91	223.8
3	92.6	0.672	0.68	187.8	166.3	0.89	182.2
4	128.2	0.534	0.56	137.4	130.8	0.95	150.3
5	86.0	0.702	0.73	193.5	175.4	0.91	182.8
6	109.6	0.598	0.60	161.1	142.3	0.88	155.0
7	148.1	0.474	0.50	137.7	119.2	0.87	132.9
8	205.1	0.359	0.38	114.1	107.1	0.94	126.0
9	107.5	0.606	0.62	159.8	143.5	0.90	154.9
10	137.0	0.505	0.52	140.7	123.3	0.88	134.8
11	185.2	0.392	0.40	126.7	109.3	0.86	117.4
12	256.4	0.293	0.30	108.7	102.1	0.94	106.7
13	129.0	0.528	0.55	142.1	126.9	0.89	138.0
14	164.4	0.434	0.45	129.8	113.4	0.87	120.2
15	222.2	0.334	0.35	120.7	104.0	0.86	113.6
16	161.3	0.441	0.45	128.0	113.6	0.89	118.4
17	205.5	0.357	0.37	121.0	105.4	0.87	106.3
18	277.8	0.272	0.28	115.8	99.8	0.86	100.6
19	384.6	0.200	0.20	103.6	97.3	0.94	93.2
20	333.3	0.229	0.23	113.3	97.5	0.86	93.9
21	461.5	0.168	0.18	102.3	95.9	0.94	92.6
22	215.1	0.343	0.36	117.2	103.5	0.88	103.1
23	274.0	0.275	0.28	114.3	99.4	0.87	96.3
24	370.4	0.207	0.21	112.1	96.6	0.86	92.9
25	512.8	0.151	0.16	101.7	95.4	0.94	91.9

List of Figures